

Supporting Information

Zn (II)-Coordination-driven Self-assembled Nanoagents for Multimodal Imaging-Guided Photothermal/Gene Synergistic Therapy

Hui Hu,^{†a} Nan Yang,^{†b} Jiahui Sun^a, Fu Zhou^a, Rui Gu^b, Yuan Liu^a, Li Wang^a, Xuejiao Song^b, Ruirui Yun^a, Xiaochen Dong,^{*b} and Guangfeng Wang^{*a}

^aKey Laboratory of Chem-Biosensing, Anhui Province; Key Laboratory of Functional Molecular Solids, Anhui Province, College of Chemistry and Materials Science, Anhui Normal University, Wuhu 241000, China

E-mail: wangyuz@mail.ahnu.edu.cn

^bKey Laboratory of Flexible Electronics (KLOFE) and Institute of Advanced Materials (IAM), Nanjing Tech University (NanjingTech), Nanjing 211816, China

E-mail: iamxcdong@njtech.edu.cn

†These authors contributed equally to this work.

Experimental Section

Materials and methods

Zinc nitrate hexahydrate, IR 780, and 2-methylimidazole were obtained from Sinopharm Chemical Reagent Co., Ltd. The sodium phosphate monobasic and sodium phosphate dibasic were purchased from Shanghai Yuanye Bio-Technology Co., Ltd. Roswell Park Memorial Institute 1640 (RPMI 1640), fetal bovine serum (FBS), penicillin/streptomycin, phosphate buffer (PBS), the cell counting kit-8 (CCK-8), the Hoechst 33342, propidium iodide (PI) and calcein acetoxymethyl ester (Calcein AM) were purchased from Beyotime Biotechnology Co., Ltd. The siRNAs and RNase A were acquired from Sangon Biotech Co., Ltd. (Shanghai, China).

siRNA: 5'-CGACGGAGACAAGCCCAAGdTdT-3'

FAM-labeled-siRNA: 5'-FAM-CGACGGAGACAAGCCCAAGdTdT-3'

Aptamer: 5'-TTGGTGGTGGTGGTTGTGGTGGTGGTGG-3'

Apparatus

Mass Spectroscopy (MS) measurements were performed on a Quattro Premier XE system (Waters) with an electrospray interface. ¹H NMR spectra were recorded on Bruker AV400 spectrometers using solvent as internal standard at room temperature. Transmission electron micrographs (TEM) were obtained using the field emission transmission electron microscope (Hitachi HT7700, Japan). Powder X-ray diffraction experiments (XRD) were performed on PANalytical X'Pert diffractometer with Cu K α irradiation. Fourier-transform infrared spectra (FT-IR) were recorded on an FT-IR-8400S spectrometer (Shimadzu, Japan) using the KBr pellet technique. Thermogravimetry (TG) was carried out on a Netzsch Thermoanalyzer STA 409 instrument in an atmospheric environment with a heating rate of 10 °C min⁻¹. The X-ray

photoelectron spectra (XPS) were taken on an ESCALAB 250Xi XPS (Thermo Fisher Scientific, USA) electron spectrometer. The hydrodynamic particle sizes and zeta potential values were examined on the Malvern Zetasizer Nano ZS series instrument. Fluorescent spectrum analyses were performed on a Luminous spectrofluorometer (Thermo Fisher Scientific, China). The quartz cuvette has a thickness of 1 cm, and both excitation and emission slits were set at 5.0 nm with a 500 V PMT voltage. Under ambient conditions, the confocal fluorescence images were acquired with a confocal laser scanning microscopy (Olympus FluoView 1000, Japan).

Synthesis of the designed IR 780-1

5-aminoisophthalic acid (a) (10 g, 55 mM) was added to 100 mL of anhydrous ethanol and sulfoxide chloride thionyl chloride (12 mL, 165 mM, 3 equiv) was dropped at 0 °C. After dripping, the mixture was heated and refluxed for 5 h, and the ethanol solution was removed by vacuum distillation. The crude product was dissolved in ethyl acetate, washed with saturated sodium bicarbonate aqueous solution, dried by adding anhydrous sodium sulfate, and the solvent was distilled off under reduced pressure to obtain a solid white product (b). Then, (b) (2.0 g, 10.6 mM, 1 equiv) in 170 mL hydrochloric acid solution (6 M) and the sodium sulfite (870 mg, 12.7 mM, 1.2 equiv) were dissolved in 2 mL water solution at the temperature below 5 °C. The potassium iodide (2.6 g, 16 mM, 1.5 equiv) was added to 10 mL of water and dropwise to the stirring solution. After the dropwise addition, the resulting mixture was warmed to room temperature and stirred for 4 h. After completion of the reaction, the solution was added to a separatory funnel. The organic phase obtained by extracting twice with dichloromethane was washed twice, dried, and then distilled under reduced pressure to remove the solvent. The eluent composed of petroleum ether and ethyl acetate was purified by silica gel flash column

chromatography to obtain a pale yellow solid (c). The product (c) (5.0 g, 23 mM, 1 equiv) was dissolved in 20 mL piperidine and trimethylsiloxane (3.9 mL, 27.4 mM, 1.2 equiv) were added. Pd(PPh₃)₄ (658 mg, 0.57 mM, 2.5 mol %) and cuprous iodide (43 mg, 0.23 mM, 1 mol %) were added at 0 °C. After stirring for 3 h at room temperature, it was quenched with saturated aqueous ammonium chloride solution, and then the mixture was added to a separatory funnel extracted twice with dichloromethane. The organic phase was collected and washed with brine, dried by adding anhydrous sodium sulfate, and the solvent was distilled off under reduced pressure. Using the eluent composed of petroleum ether and dichloromethane, purified by silica gel flash column chromatography to obtain a light yellow solid (d). Then (d) (3.0 g, 9.4 mM, 1 equiv) was dissolved in a mixed solution of ethanol/dichloromethane (1:1 volume ratio), Cesium carbonate (3.4 g, 10 mM, 1.1 equiv) was added, the solution was stirred at room temperature for 1 h, and the solvent was removed by distillation under reduced pressure. The remaining crude product was scatted in a mixed solution of water/dichloromethane (1:1 volume ratio) and added in a separatory funnel, repeating the same extraction, drying, and distillation steps as described above, and purified by silica gel flash column chromatography using dichloromethane as the eluent, a light yellow solid (e) was obtained.

The purchased IR 780 dye (1 g, 1.49 mM, 1 equiv), 5-ethynyl terephthalate (e) (1.46 g, 5.96 mM, 4 equiv), Pd(PPh₃)₂Cl₂ (104 mg, 0.15 mM, 2.5 mmol%), PPh₃ (77 mg, 0.3 mM, 5 mmol%) and CuI (56 mg, 0.3 mM, 5 mmol%) were mixed in a 100 mL two-neck solvent bottle, connected the reaction flask to a double-row tube with a vacuum pump. Turning on the vacuum pump to evacuate and pass in high-purity argon, then 5 mL of anhydrous triethylamine and 5 mL of DMF solution were added while passing in argon, and the mixture was heated to 80 °C for 5 h. After

the organic solvent was distilled off under the reduced pressure, dichloromethane/methanol (1:1 volume ratio) was used as an eluent and purified by silica gel flash column chromatography to obtain a purple final solid product (f, named as IR 780-1).

Synthesis of siRNA@PT-ZIF-8

siRNA@PT-ZIF-8 was synthesized via a one-pot self-assembly approach. Briefly, a mixture of IR 780-1 (1.5 mg) and 2-methylimidazole (4.1 mg) in 300 μL methanol was added to the water at room temperature. Then, 200 μL siRNA (input concentration 1.0 mg mL^{-1}) were quickly added, and the mixture was stirred for one hour, followed by the slow addition of 500 μL zinc nitrate solution (2.98 mg) under mechanical agitation. After that, the product was left to stand for another 24 h and isolated by centrifugation at 13000 rpm for 30 min. Finally, the powdered siRNA@PT-ZIF-8 was obtained by freeze-drying. For in vitro or in vivo study, siRNA@PT-ZIF-8 was dissolved in 1 \times PBS (10 mM, pH = 7.4) at specific concentrations.

PT-ZIF-8 or siRNA@ZIF-8 was prepared under the same conditions as the above, except that no siRNA or PT ligand was added. Besides, washed and centrifuged by mixing 200 μL aliquot of 500 nM siRNA with the freshly prepared PT-ZIF-8 in methanol (2.0 mg/mL), the resulting solution was incubated for 30 min, washed, and centrifuged to obtain siRNA+PT-ZIF-8.

Preparation of the aptamer modified siRNA@PT-ZIF-8 (Apt/siRNA@PT-ZIF-8)

To immobilize the aptamer on siRNA@PT-ZIF-8, the nucleolin aptamer aqueous solution (5 μM) was quickly added to the siRNA@PT-ZIF-8 aqueous solution (1 mg/mL). After that, the mixed solution was heated to 37 $^{\circ}\text{C}$ and vibrated for 12 h to obtain Apt/siRNA@PT-ZIF-8.

siRNA@PT-ZIF-8 mediated siRNA release

To quantify siRNA release, 1.0 mg/mL siRNA@PT-ZIF-8 was dispersed in 10 mM PBS buffer with different pH values (pH = 7.4 and 5.5). At the set time intervals, aliquots from different treatments were centrifuged, and 200 μ L of the released FAM-siRNA in the suspensions were collected by centrifuging at 13000 rpm for 10 min. The amount of siRNA or IR780-1 in the supernatant was further measured by fluorescent spectroscopy (siRNA excitation/emission wavelength: 488 nm/525 nm; IR780-1 excitation/emission wavelength: 552 nm/625 nm) by a standard curve method, while the loading capacity (LC) and loading efficiency (LE) were calculated using the following equations.

$$\text{Loading capacity} = m_{\text{loaded}}/m_{\text{siRNA@PT-ZIF}} \times 100\%$$

$$\text{Loading efficiency} = m_{\text{loaded}}/m_{\text{feeding}} \times 100\%$$

The measured loading capacity of IR780-1 or siRNA in the siRNA@PT-ZIF-8 increased along with the rise of the fed amount of IR780-1 (0.2, 0.5, 1.0, 1.5, 2.0 mg mL⁻¹) or siRNA (~0.2, 0.5, 1.0, 2.0 mg mL⁻¹). Finally, it reached a maximum loading capacity of 21.0% and 12.5% at an IR780-1 amount of 1.5 mg/mL and siRNA 1.0 mg/mL, respectively.

1.0 mg/mL siRNA@PT-ZIF-8 in 10 μ L PBS solution with different pH values (10 mM, pH 7.4 and pH 5.5) was mixed with 100 U/mL of RNase A (10 μ L) and incubated for 30 min at 37 $^{\circ}$ C to evaluate the protective effect of siRNA@PT-ZIF-8 to siRNA. Then, 2 μ L EDTA (100 mM) was added to inactivate RNase A and centrifuged at 8000 rpm for 5 min. The collected solids were re-suspended in 20 μ L of an aqueous solution for following agarose gel electrophoresis. More specifically, 10 μ L of sample solution was mixed with 6 \times loading buffer (2 μ L) and then injected into the pockets. Then electrophoresis was carried out at a constant voltage of 100 V

for 60 minutes, followed by staining with GelRed for 20 minutes. Finally, the gel was imaged by JS 680-D (Peiqing, Shanghai) under UV irradiation.

In vitro photothermal performance of the siRNA@PT-ZIF-8

The siRNA@PT-ZIF-8 solutions of different concentration (0, 10, 20, 30, 40 $\mu\text{g/mL}$) were irradiated with an 808 nm laser ($2.0 \text{ W}\cdot\text{cm}^{-2}$) in 10 mM PBS (pH = 7.4). And the temperature changes were recorded by using a digital thermometer. IR thermal images were obtained with an IR thermal camera at a certain time interval. To study the thermal stability of siRNA@PT-ZIF-8, the siRNA@PT-ZIF-8 aqueous suspensions (50 $\mu\text{g/mL}$) were first exposed to 808 nm laser irradiation ($2.0 \text{ W}\cdot\text{cm}^{-2}$) for 5 min. Then, the solutions were naturally cooled down to room temperature. This process was successively repeated five times under the same condition. And the photothermal conversion efficiency of the siRNA@PT-ZIF-8 was calculated according to the formula as follows:

$$\eta = \frac{\frac{m_D c_D}{\tau_s} (T_{max} - T_{surr}) - Q_s}{I(1 - 10^{-A})}$$

Where T_{max} means the equilibrium temperature, T_{surr} is the ambient temperature of the surroundings. τ_s is the sample-system time constant, m_D and c_D are the solvent's mass and heat capacity ($4.2 \text{ J}\cdot\text{g}^{-1}$). The Q_s expresses the heat associated with light absorption by the solvent. The I represents incident laser power ($2.0 \text{ W}\cdot\text{cm}^{-2}$), A is the absorbance of samples at 808 nm.

Cell culture and cellular uptake

The 4T1 cells were cultured in RPMI 1640 medium containing 10% FBS and 0.1% penicillin-streptomycin at $37 \text{ }^\circ\text{C}$ in a humidified 5% CO_2 atmosphere. The cell counter calculated the cell number. For cellular uptake studies, the 4T1 cells were seeded in 96 wells plate at a density of

5.0×10^5 cells. After that, the free IR 780-1, as-prepared siRNA@PT-ZIF-8 and Apt/siRNA@PT-ZIF-8 ($50 \mu\text{g mL}^{-1}$, with the same concentration of $\sim 6.25 \mu\text{g mL}^{-1}$ of siRNA and $\sim 10 \mu\text{g mL}^{-1}$ IR780-1) were added to the wells at 37°C with incubation for 12 h, respectively. After rinsing with PBS three times, the fluorescence was observed by CLSM from 505 to 545 nm with excitation at 488 nm for FAM and 600 to 650 nm with excitation at 552 nm for IR 780-1. Meanwhile, the cellular uptake of different groups was also analyzed by flow cytometry.

Evaluation of cytotoxicity

The cytotoxicity for 4T1 cells with different treatments was determined by CCK-8 analysis. Briefly, 4T1 cells (1.0×10^5) were seeded in a 96-well plate for 24 h. After cell attachment, PT-ZIF-8, siRNA@PT-ZIF-8, or Apt/siRNA@PT-ZIF-8 with different concentrations (0, 10, 20, 30, 40, and $50 \mu\text{g mL}^{-1}$) was added to the medium, and the cells were incubated in 5% CO_2 at 37°C for 24 h. Then the medium was discarded, and the prepared culture medium containing 10% CCK-8 solution was added into each well at 37°C , including a negative control of the culture medium alone. After 12 hours of incubation, the absorbance was measured at 450 nm to calculate the cell viability, which the control group normalized without any treatment. Similarly, PBS + NIR, PT-ZIF-8 + NIR, siRNA@PT-ZIF-8 + NIR, and Apt/siRNA@PT-ZIF-8 + NIR groups were treated with laser irradiation (2.0 W cm^{-2} , 808 nm) for 5 mins after 10 hours of incubation. The absorbance was measured at 450 nm for another 2 hours.

The cytotoxicity for human cervical carcinoma Hela cell, mouse pulmonary fibroma L929 and human alveolar epithelium cells A549 treated with Apt/siRNA@PT-ZIF-8 NPs were also determined by CCK-8 analysis.

Live/dead cell staining assay

4T1 cells were seeded into confocal plates at the density of 1.0×10^5 cells per well and incubated at 37 °C for 24 h. Then, the culture medium was replaced with the fresh RPMI 1640 with specific concentrations of different nanocomposites and incubated continuously for about 12 h in dark conditions. After 808 nm laser ($2.0 \text{ W}\cdot\text{cm}^{-2}$) for 5 min irradiation, the cells were further cultured for 4 hours. Subsequently, the treated plates were washed with PBS, and the mixture of calcein-AM (1 μM) and PI (3 μM) was used to stain the live/dead cells. After 20 min of incubation, the residual dyes were removed by PBS three times. Next, the resulting cells were imaged by CLSM, where the green fluorescence was collected at 488 nm, and the red fluorescence was collected at 543 nm. Furthermore, the groups pre-incubated with Annexin V-FITC and PI dyes were analyzed by flow cytometry.

Western blot assay

4T1 cells were seeded into a 6-well plate (5×10^6 per well) and incubated at 37 °C overnight. Then different formulas were added to the wells for 12 hours: (1) Apt/siRNA@PT-ZIF-8 + NIR, (2) PBS, (3) PBS + NIR, (4) siRNA, (5) PT-ZIF-8, and (6) PT-ZIF-8 + NIR. The group with laser irradiation was irradiated (808 nm , 2 W cm^{-2}) for 5 min. Then, cells were cultivated for another 2 h and extracted for western blotting. Glyceraldehyde-3-phosphate dehydrogenase (GAPDH) was used as an internal reference protein. Heat shock protein (HSP) was a type of heat emergency protein that exists widely in organisms (such as HSP60, HSP70, HSP90, etc.). When it was stimulated by high temperature, hypoxia, etc., the expression level would increase rapidly.

Tumor models

All animal experiments were approved and guided by the School of Pharmaceutical Science, Nanjing Tech University, in compliance with the relevant laws and institutional guidelines. The female Balb/c mice and nude mice (16-18 g, 4-5weeks) were purchased from the Comparative Medicine Centre of Yangzhou University. The 4T1 cells were inoculated on the right rear leg of the Balb/c mice with 50 μL of PBS containing 4.0×10^6 4T1 cells. When the tumor volumes approached 100-150 mm^3 , the mice were used to carry out the following in vivo experiments.

Apt/siRNA@PT-ZIF-8 mediated fluorescence/photoacoustic/photothermal imaging

For in vivo fluorescence imaging (FI), the Balb/c mice bearing tumor (4T1 cells) were injected by tail vein with PBS (200 μL) or 200 μL Apt/siRNA@PT-ZIF-8 (400 $\mu\text{g}/\text{mL}$, IR780-1 $\sim 0.8 \text{ mg Kg}^{-1}$). At 0, 2, 4, 8, 12, and 24 h post-injection, mice were anesthetized for imaging by the fluorescence-imaging instrument.

The 4T1-bearing nude mice models were intravenously injected with 200 μL Apt/siRNA@PT-ZIF-8 (400 $\mu\text{g}/\text{mL}$, IR780-1 $\sim 0.8 \text{ mg Kg}^{-1}$) to measure the in vivo photoacoustic (PA) signals at the tumor site. Then the mice were put into the LOIS-3D machine to collect the PA signals of the tumor at different times (0, 2, 4, 8, 12, and 24 h) under an 808 nm laser.

The in vivo photothermal conversion properties were investigated using a FLIR thermal camera. Significantly, the mice with tumors were injected with PBS (200 μL) or 200 μL Apt/siRNA@PT-ZIF-8 (400 $\mu\text{g}/\text{mL}$, IR780-1 $\sim 0.8 \text{ mg Kg}^{-1}$). After 8 h, the tumor region was irradiated with an 808 nm laser, and a FLIR thermal camera recorded the variation of temperature and images with exposure times ranging from 0 to 10 min.

In vivo antitumor efficiency

The 4T1 tumor-bearing mice with a tumor size of 125 mm³ were randomly divided into six groups (n = 4 for each group) for various treatments: (1) PBS, (2) PBS + NIR, (3) siRNA@PT-ZIF-8, (4) siRNA@PT-ZIF-8 + NIR, (5) Apt/siRNA@PT-ZIF-8, (6) Apt/siRNA@PT-ZIF-8 + NIR. The mice of the control group were injected with PBS (200 μL), and other groups were injected with 200 μL nanocomposites dispersion solution (400 μg/mL, IR780-1 ~0.8 mg kg⁻¹, siRNA ~0.5 mg kg⁻¹). After 8 h of injection, the whole tumor region was irradiated with an 808 nm laser (2.0 W·cm⁻², 5 min). Mice were treated every 2 days and repeated 3 times. The average temperature in the tumor region was monitored using an infrared thermal imaging system. Bodyweight changes and tumor volumes of each group were observed and recorded every two days by a digital scale and caliper, respectively. The tumor volume was obtained as the following formula: tumor volume = $a \times b^2/2$, where a is tumor length and b is tumor width. For the H&E analysis, these organs were embedded into the paraffin, stained by hematoxylin solution and eosin solution. The sections were observed by CLSM.

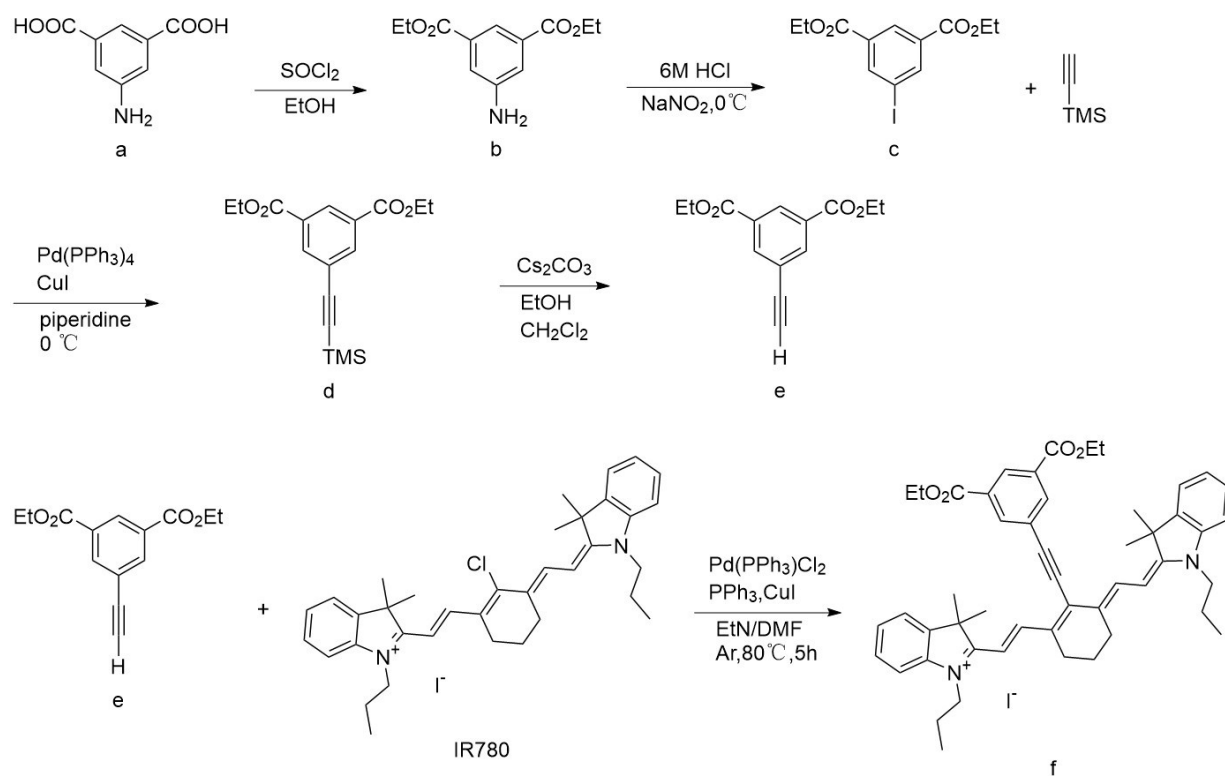
Long-Term Toxicity Assessment in vivo

Healthy Balb/c mice were intravenously administrated with PBS and APT/siRNA@PT-ZIF-8 (siRNA@PT-ZIF-8: 4 mg kg⁻¹) to evaluate the long-term toxicity of the obtained formulation. Then 1 mL of blood from each mouse was collected for the blood biochemistry analysis at 0, 3, 7, and 15 days post-injection. Liver function was tested by measuring serum levels of ALP (alkaline phosphatase), ALB (albumin), and ALT (glutamate transaminase). Kidney function was evaluated by determining BUN (blood urea nitrogen) and CREA (creatinine). Heart function markers were measured: creatine kinase (CK), creatine kinase isoenzyme (CK-MB), and lactate dehydrogenase 1 (LDH1).

Statistical Analysis: Quantitative data were exhibited as means \pm standard deviation and performed by ANOVA. One-way ANOVA analyzed differences among multiple groups. Student-Newman-Keuls test was utilized as a post hoc test. $P < 0.05$ was identified to be statistically significant.

The synthetic route for IR 780-1

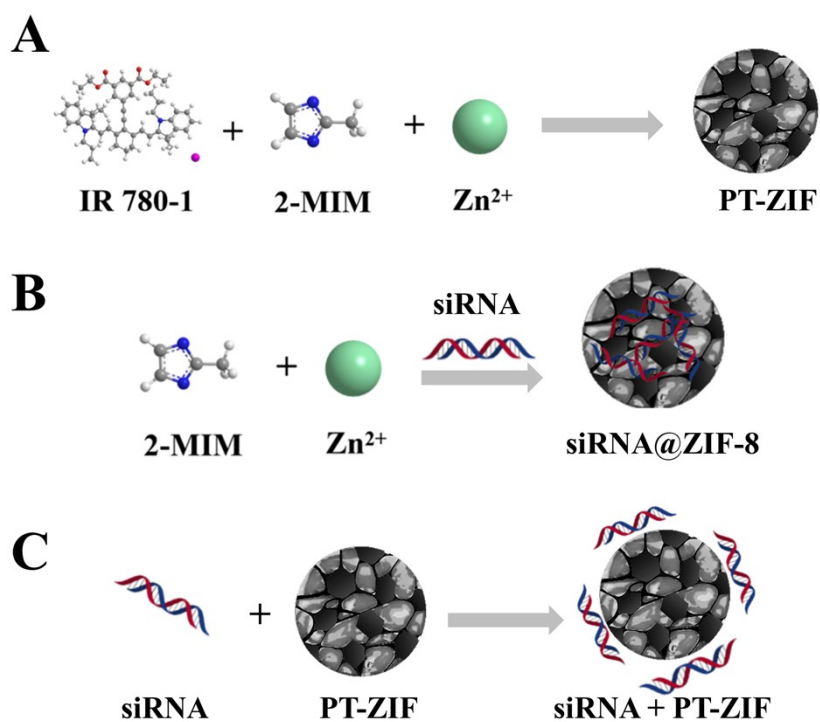
To functionalize the NIR organic dye IR 780 with the coordination sites, 5-ethynyl terephthalate was designed and synthesized with 5-Aminoisophthalic acid as raw material. Furthermore, it was conjugated with IR 780 by a one-step Pd-catalyzed reaction to obtain IR 780-1.



Scheme S1. The synthetic route for IR 780-1.

Schematic illustration of the control nano vehicles synthesis

To investigate the role of photothermal ligand of IR 780-1 and siRNA and the encapsulation effect, the corresponding nano vehicles were synthesized. Without the addition of siRNA or IR 780-1, PT-ZIF-8 or siRNA@ZIF-8 was obtained (Figure S1 A, B). Besides, by physical mixing siRNA with the prepared PT-ZIF-8, siRNA + PT-ZIF-8 was obtained.



Scheme S2. The schematic synthesis route for PT-ZIF-8 (A), siRNA@ZIF-8 (B), and siRNA + PT-ZIF-8 (C).

^1H NMR of IR780-1

^1H NMR (400 MHz, CDCl_3) δ 8.73 – 8.72 (m, 1H), 8.64 (dt, $J = 10.4, 1.6$ Hz, 1H), 8.30 (dd, $J = 39.2, 1.6$ Hz, 1H), 8.17 (dd, $J = 13.2, 1.6$ Hz, 2H), 7.20 – 7.13 (m, 4H), 6.90 (td, $J = 7.2, 0.8$ Hz, 2H), 6.72 – 6.64 (m, 2H), 5.46 (d, $J = 13.2$ Hz, 2H), 4.47 – 4.38 (m, 4H), 3.64 (t, $J = 7.2$ Hz, 4H), 2.65 – 2.56 (m, 4H), 1.91 – 1.81 (m, 2H), 1.76 (q, $J = 7.4$ Hz, 4H), 1.67 (s, 12H), 1.46 – 1.38 (m, 6H), 1.00 (t, $J = 7.2$ Hz, 6H).

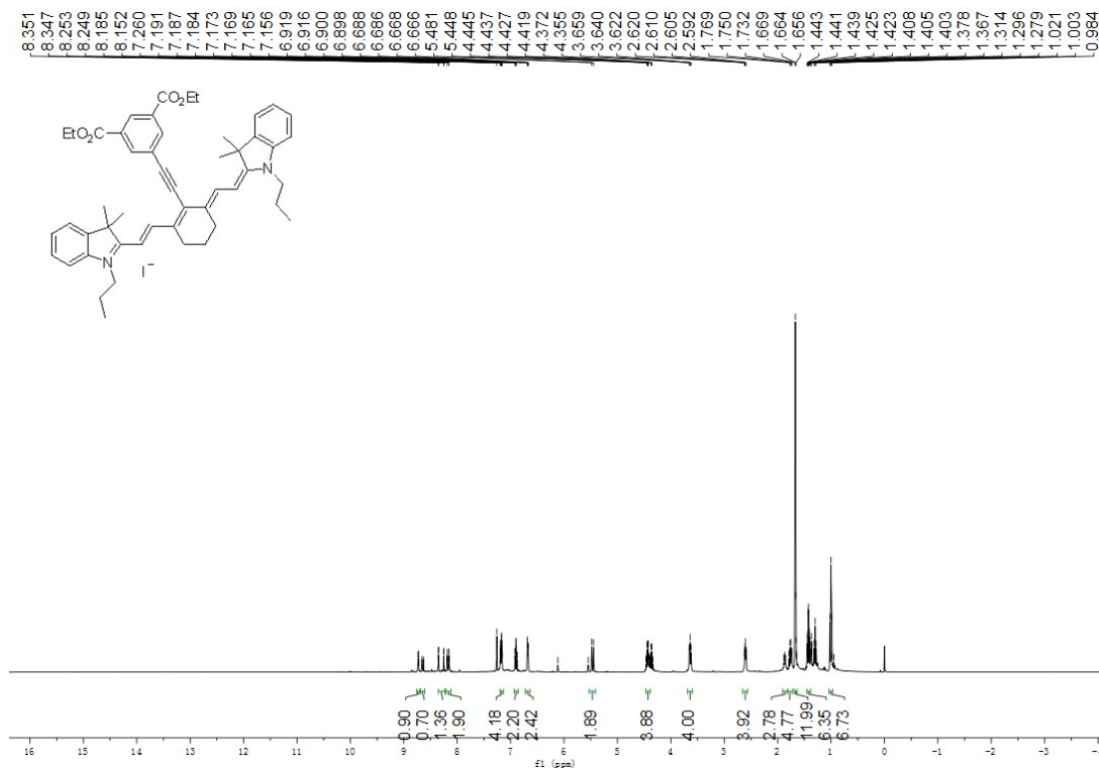


Figure S1. The ^1H NMR of IR 780-1.

¹³CNMR of IR 780-1

¹³C NMR (100 MHz, CDCl₃) δ 186.48, 165.75, 165.64, 165.17, 162.55, 144.51, 139.80, 136.64, 134.16, 134.04, 133.03, 131.58, 131.43, 131.26, 127.70, 126.59, 121.87, 120.50, 106.83, 92.65, 77.48, 77.16, 76.84, 61.78, 61.67, 61.56, 46.66, 44.24, 28.90, 25.95, 22.70, 19.87, 14.47, 14.42, 14.34, 11.86.

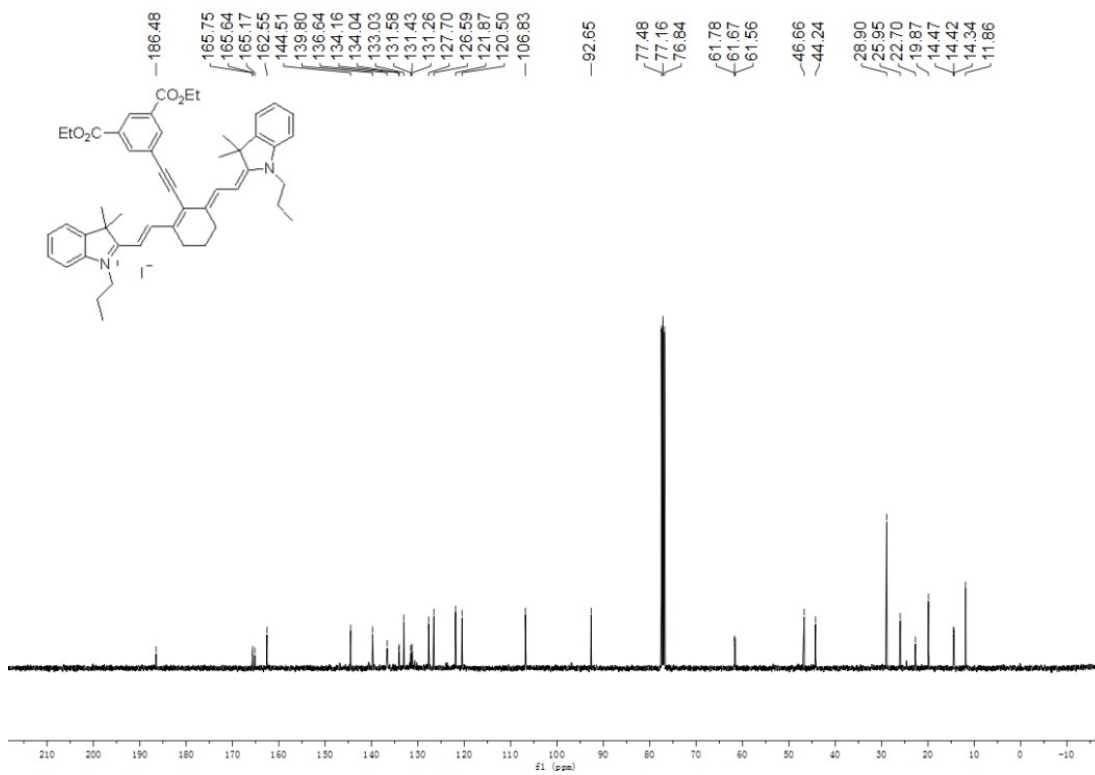


Figure S2. The ¹³C NMR of IR 780-1.

Mass spectrum of IR 780-1

MS: calculated for 2 [M+H]⁺: 750.44; obsvd. ESI-MS: m/z 750.58

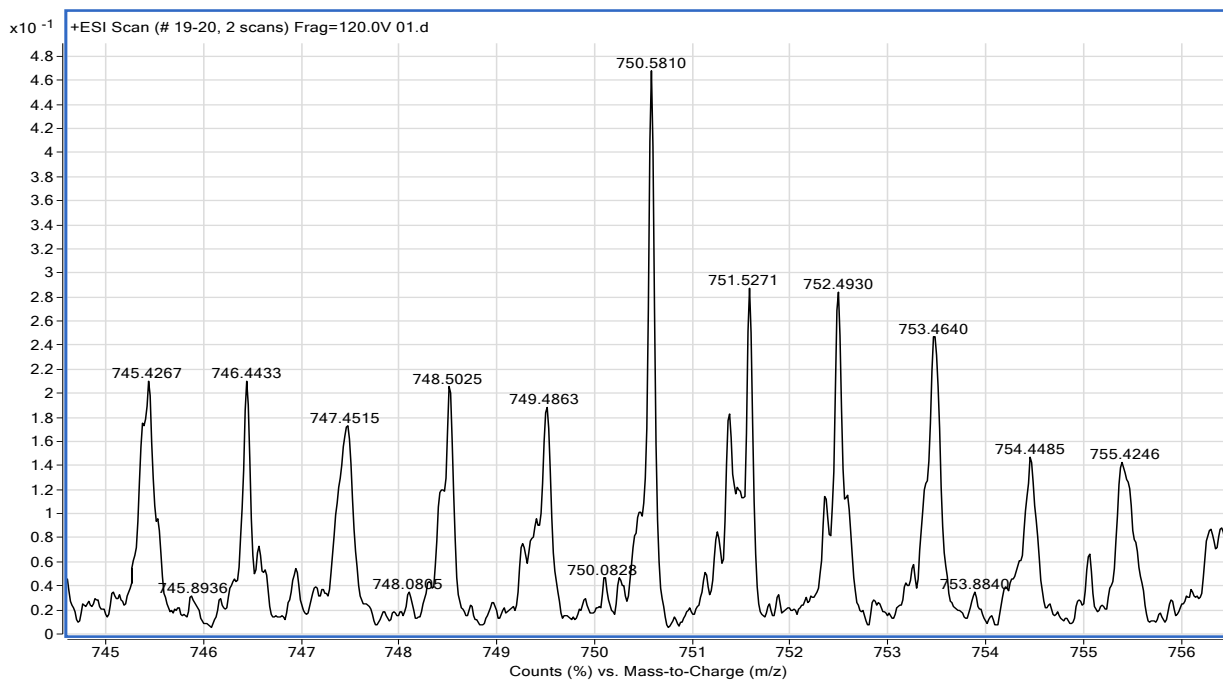


Figure S3. Mass spectrum of IR 780-1.

Elemental mapping analyses of PT-ZIF-8

The control of PT-ZIF-8 was synthesized without the encapsulation of siRNA. As shown in Figure S4, the TEM of PT-ZIF-8 had a similar shape as siRNA@PT-ZIF-8 with prominent thin film grown on the surface. However, the corresponding elemental mapping displayed a uniform distribution of N, O, C, Zn, and I except P, which was in accordance with the experimental fact.

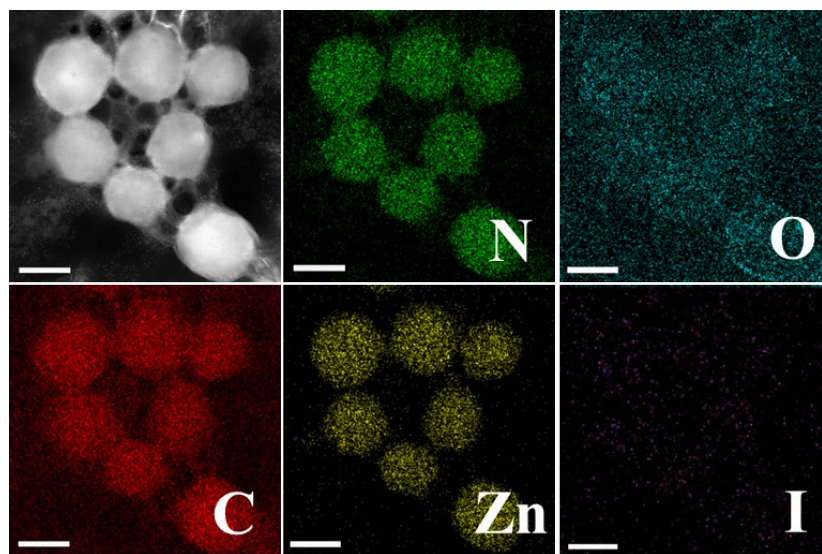


Figure S4. Elemental mapping images of PT-ZIF-8. Scale bar: 100 nm.

XPS analyses of PT-ZIF-8

The XPS wide scan of ZIF-8 and siRNA@PT-ZIF-8 and core-level of C1s, N1s, and Zn2p were studied (Figure S5). Compared with ZIF-8, the Zn2p possessed a positive shift, indicating the Zn²⁺ may coordinate with the PT ligand besides 2-MIM.

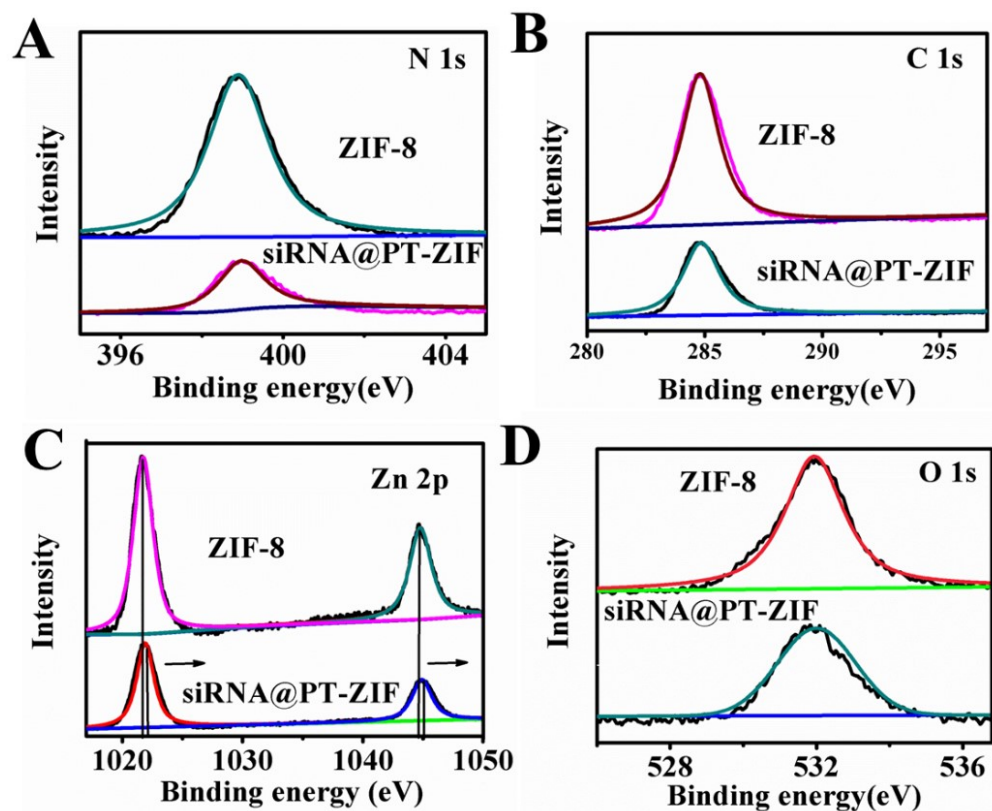


Figure S5. XPS analyses of the ZIF-8 and siRNA@PT-ZIF-8.

DLS analyses of PT-ZIF-8 and siRNA@PT-ZIF-8

As shown in Figure S6, with the siRNA encapsulation, the hydrodynamic size of siRNA@PT-ZIF-8 increased compared with that of PT-ZIF-8.

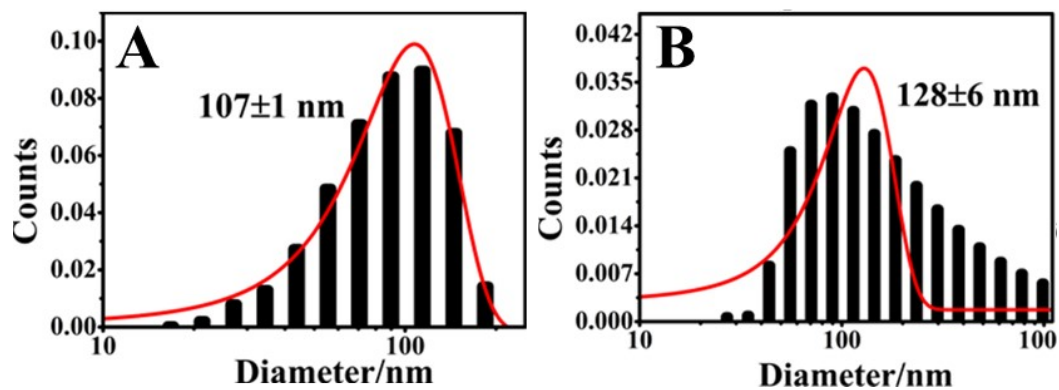


Figure S6. DLS analyses of the PT-ZIF-8 (A) and siRNA@PT-ZIF-8 (B).

CLSM photographs of siRNA + PT-ZIF-8

By physical mixing siRNA with the prepared PT-ZIF-8, siRNA+PT-ZIF-8 was obtained. The CLSM showed that nearly no green fluorescence from FAM-siRNA was observed in siRNA + PT-ZIF-8, implying the lower loading capacity of siRNA by a simple physical mixing method.

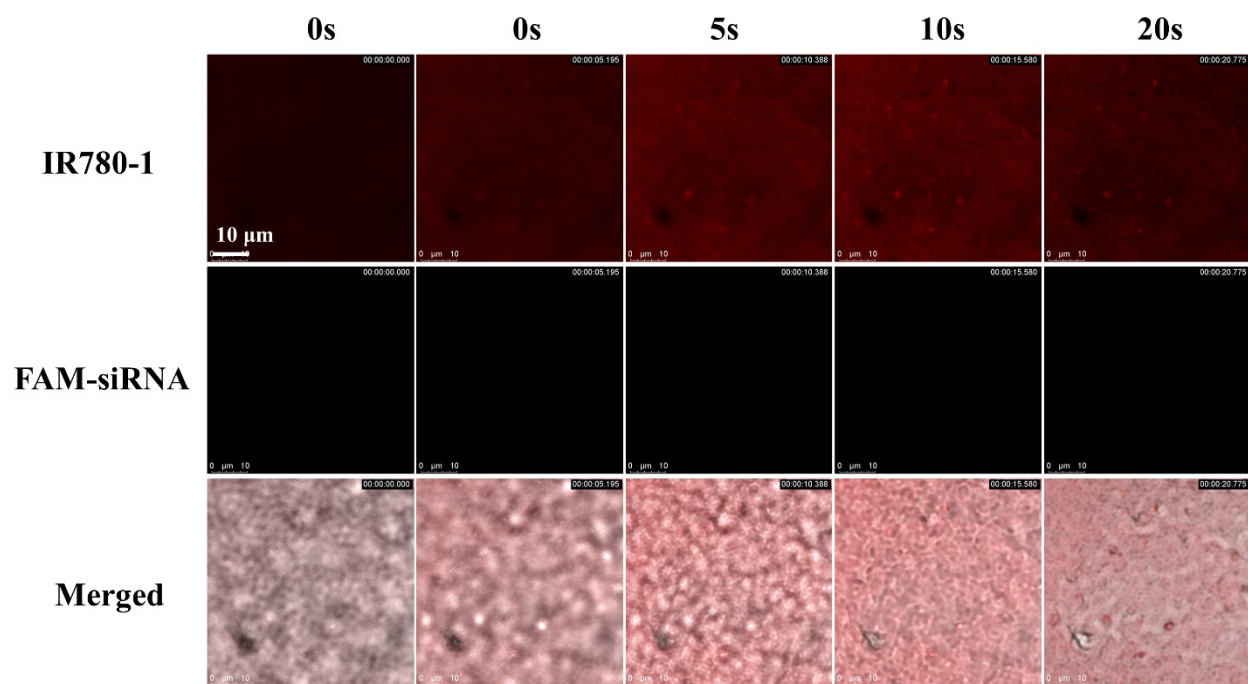


Figure S7. Layer-by-layer CLSM photographs of siRNA + PT-ZIF-8 along with the z-axis position with gradual scanning time.

DLS analyses of siRNA@PT-ZIF-8 in acid solution

As shown in Figure S8, with the incubation time increased, the DLS of siRNA@PT-ZIF-8 decreased, which may be due to the acid sensitivity of ZIF-8 skeleton induced decomposition of the nanocomposites.

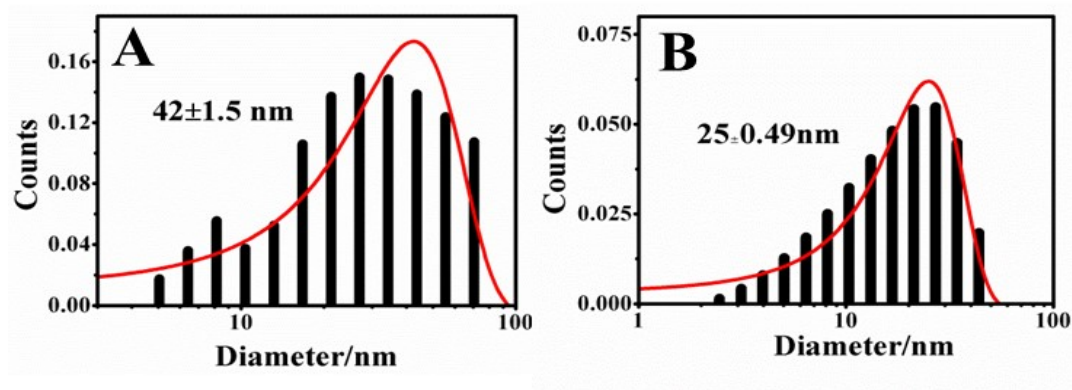


Figure S8. DLS analysis of the siRNA@PT-ZIF-8 treated with the PBS (pH=5.5) for 15 min (A) and 30 min (B).

Stability of Apt/siRNA@PT-ZIF-8

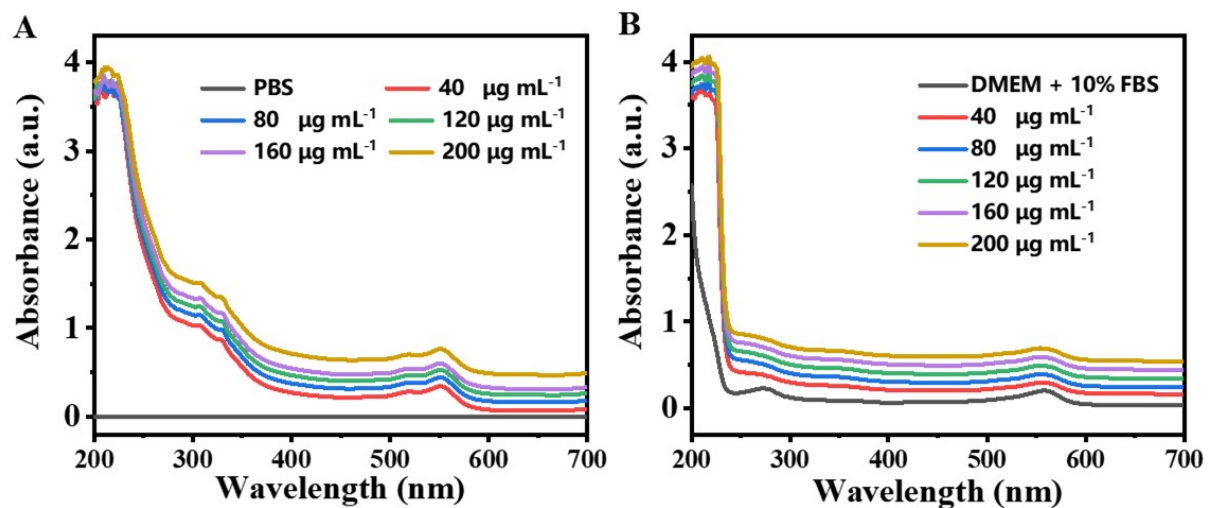


Figure S9. UV-vis absorbance spectra (A, B) in PBS (A) and DMEM containing 10% FBS (B) with different concentrations of Apt/siRNA@PT-ZIF-8 (0, 40, 80, 120, 160, 200 $\mu\text{g mL}^{-1}$) (Inset: 200 $\mu\text{g mL}^{-1}$ of the corresponding solution before and after incubation of 12 h).

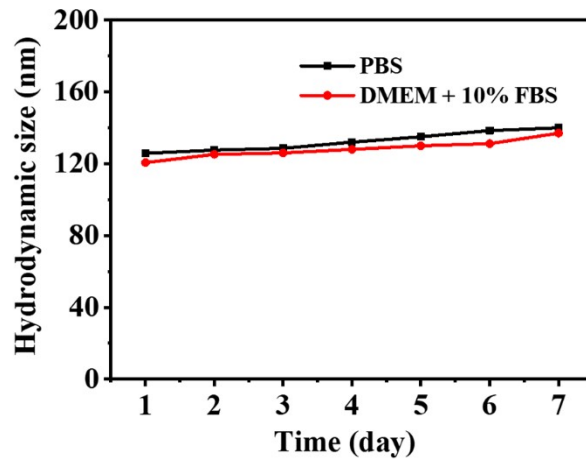


Figure S10. Hydrodynamic size of Apt/siRNA@PT-ZIF-8 in PBS (black) and DMEM containing 10% FBS (red)

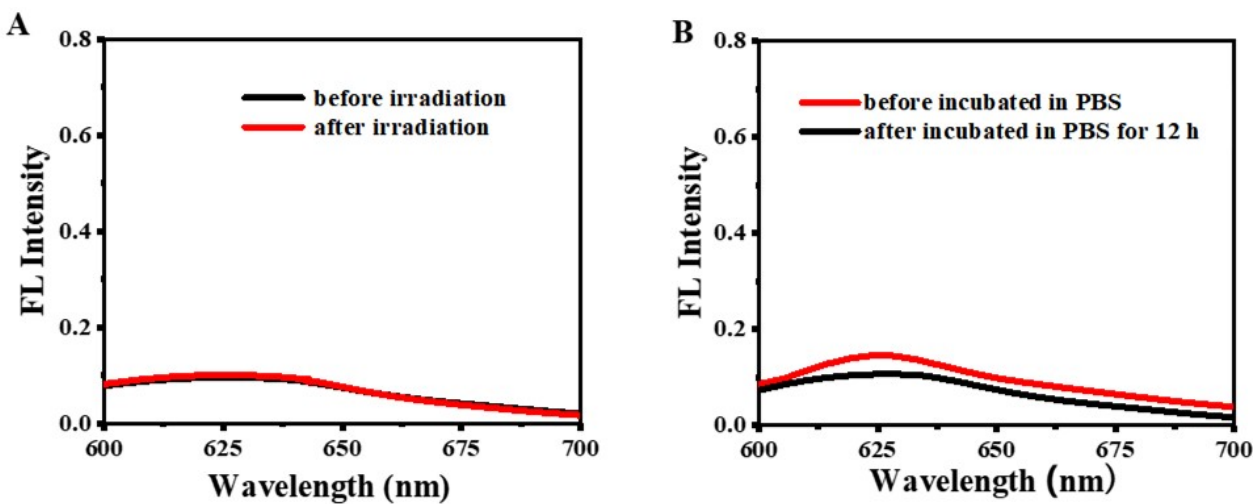


Figure S11. (A) The fluorescence spectrum of the Apt/siRNA@PT-ZIF-8 supernatant before and after the NIR laser irradiation for 5 mins. (B) The fluorescence spectrum of Apt/siRNA@PT-ZIF-8 before and after a 12 h incubation in PBS.

The degradation behavior of the Apt/siRNA@PT-ZIF-8

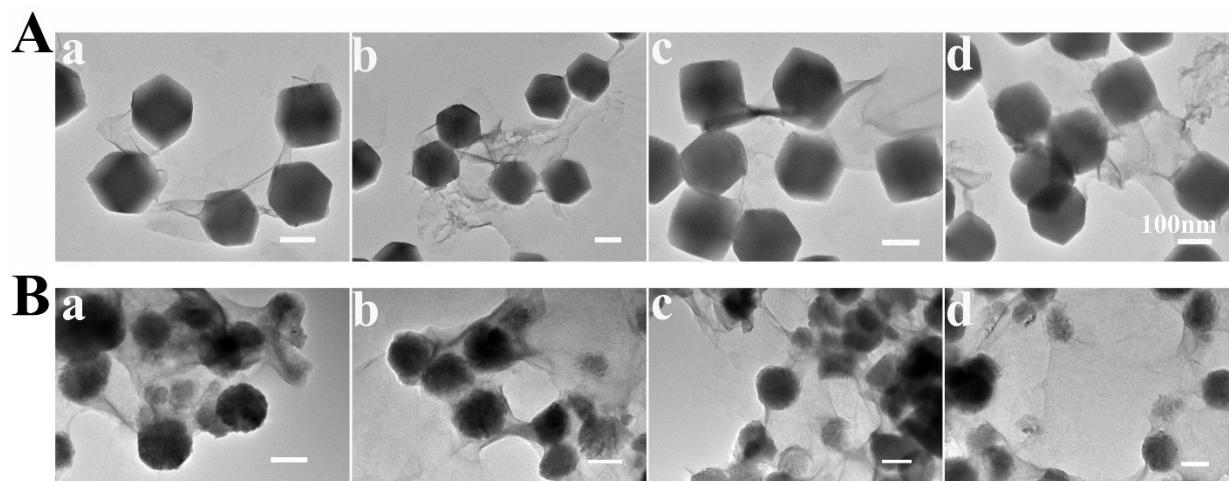


Figure S12. TEM image of Apt/siRNA@PT-ZIF-8 NPs incubated with PBS (pH 7.4) under different periods of time (a, b, c, d: 1, 3, 5, 7 days) (A) and solutions of different pH value for 5 min (a, b, c, d: pH 6.5, 6.0, 5.5, 5.0) (B).

Fluorescence spectra of siRNA@PT-ZIF-8

As shown in Figure S9, the fluorescence intensity of siRNA@PT-ZIF-8 kept no change in PBS (pH 7.4) for 180 min. However, a noticeable fluorescence increment of its supernatant was observed after it was incubated in pH 5.5 PBS for 180 min., confirming the acid triggered release of the loaded siRNA from siRNA@PT-ZIF-8.

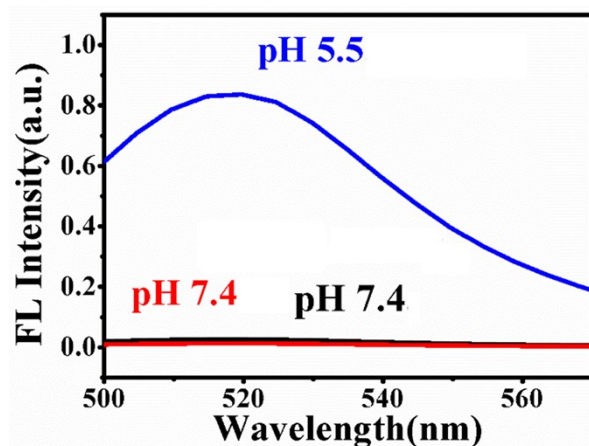


Figure S13. The corresponding fluorescence spectra of the FAM-siRNA released from $50 \mu\text{g mL}^{-1}$ siRNA@PT-ZIF-8 exposure to different pH stimuli (pH 7.4 for 0 min (red line) and 180 min (black line), and pH 5.5 for 180 min (blue line)).

Agarose gel analysis

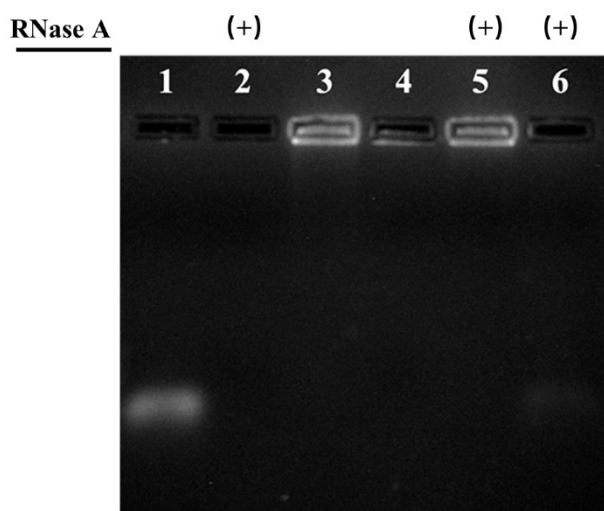


Figure S14. Agarose gel shifts of siRNA (lane 1), siRNA + RNase A (lane 2), siRNA@PT-ZIF-8 (lane 3), siRNA@ZIF-8 (lane 4), siRNA@PT-ZIF-8 at pH 7.4 (lane 5) and at pH 5.5 (lane 6) when exposed to purified RNase A.

The photothermal effect of siRNA@PT-ZIF-8

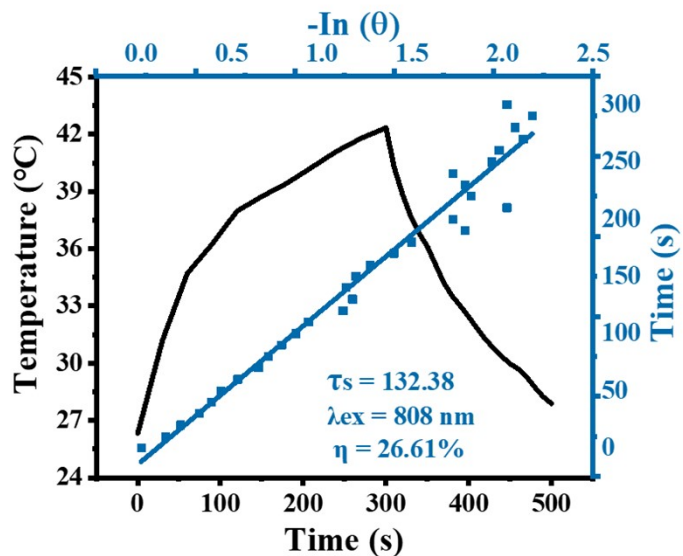


Figure S15. Heating and cooling curves of $50 \mu\text{g mL}^{-1}$ siRNA@PT-ZIF-8 upon being irradiated for 10 min (808 nm , 2 Wcm^{-2}) with the laser turned on and off (black). Linear time data from the cooling period versus the negative natural logarithm of driving force temperature (blue).

The stability of the Apt/siRNA@PT-ZIF-8



Figure S16. Fluorescence spectra of Apt/siRNA@PT-ZIF-8 supernatant before and after (A) the NIR laser irradiation (2 W cm^{-2} , 5 min), (B) incubated in PBS (pH = 7.4) for 12 h.

Fluorescent study of siRNA@PT-ZIF-8 in 4T1 cells

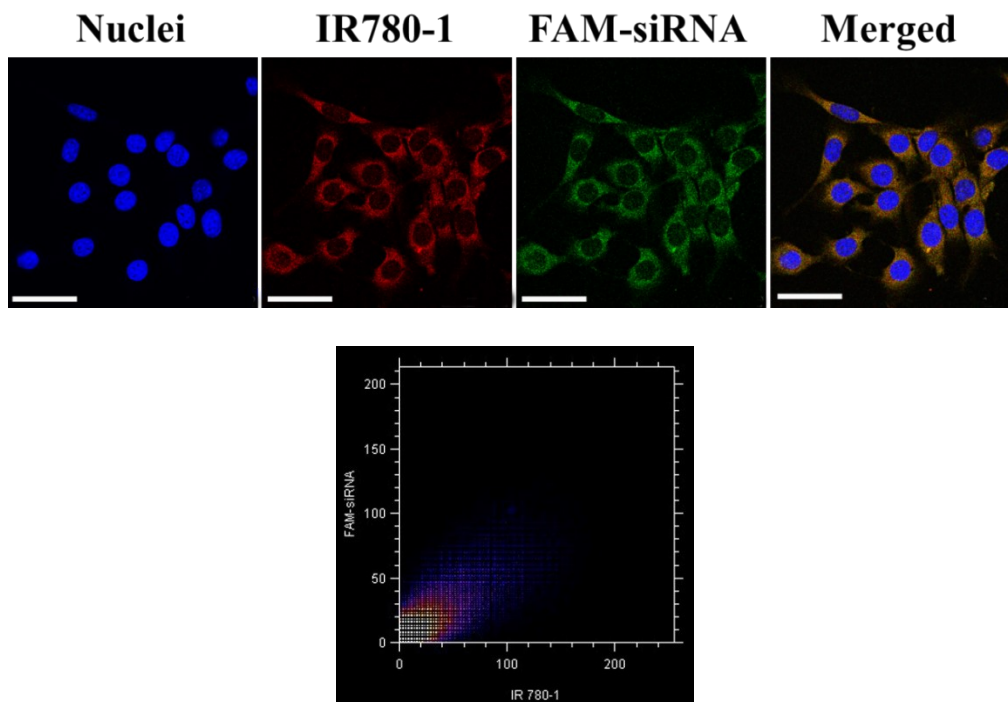


Figure S17. Fluorescent visualization of siRNA and IR780-1 localization in 4T1 cells 12 h after incubation with $50 \mu\text{g mL}^{-1}$ Apt/FAM-siRNA@PT-ZIF-8. Scale bar: $50 \mu\text{m}$.

The quantitative analyses of western blots

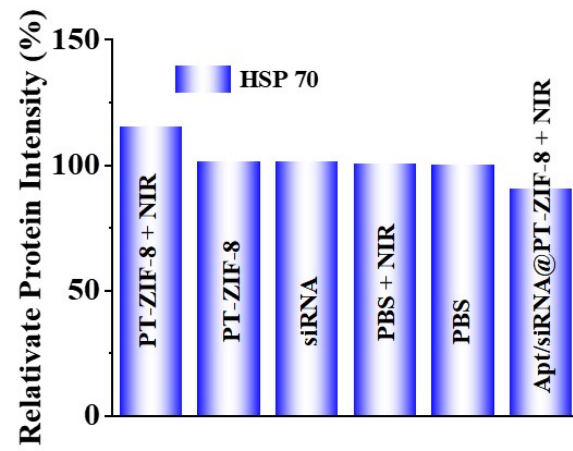


Figure S18. The quantitative analyses of HSP70.

The cytotoxicity of Apt/siRNA@PT-ZIF-8

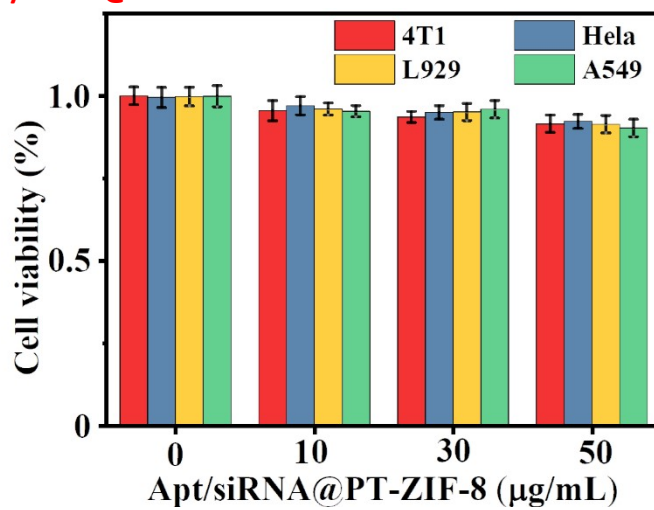


Figure S19. Cell Viability of 4T1/HeLa/L929/A549 cells treated with Apt/siRNA@PT-ZIF-8 for 12 hours.

Fluorescence images of main organs and tumor

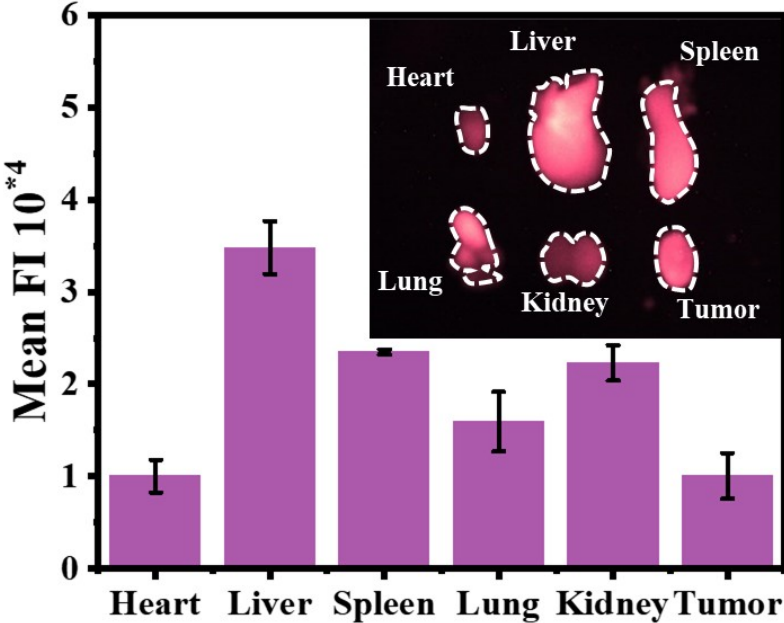


Figure S20. Fluorescence intensity and images of main organs and tumor 24 h after injection from the sacrificed mice.

Photographs of the harvested tumors

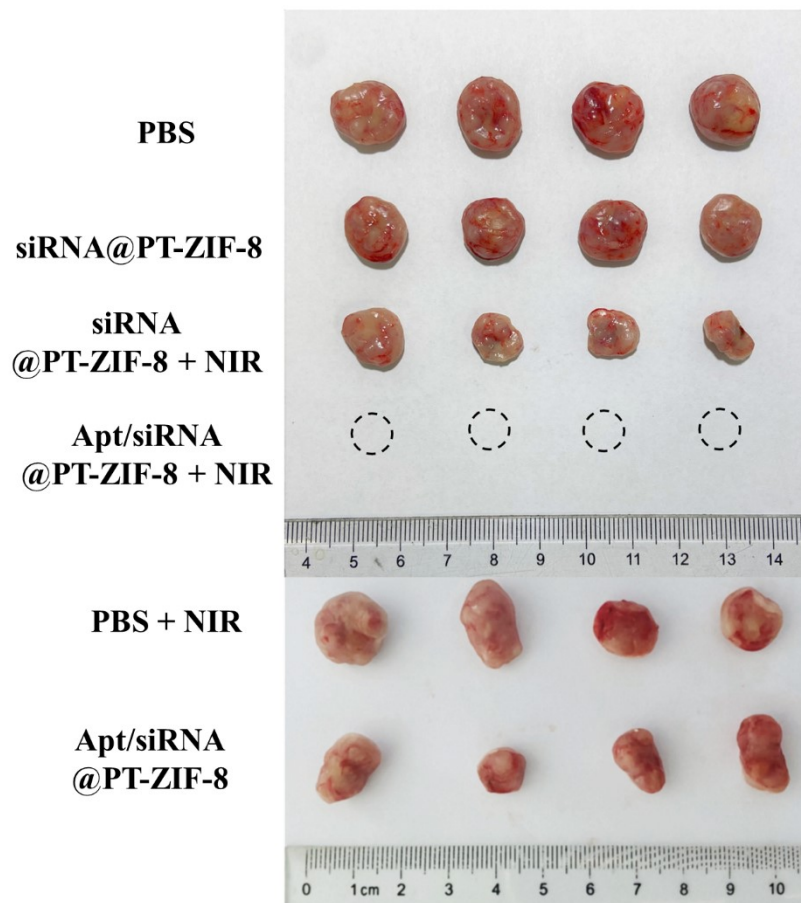


Figure S21. Photographs of the tumors in the six groups after 12 days of treatment and the blank space represent the tumor-free status.

Half-time period of Apt/siRNA@PTZIF-8 NPs in blood

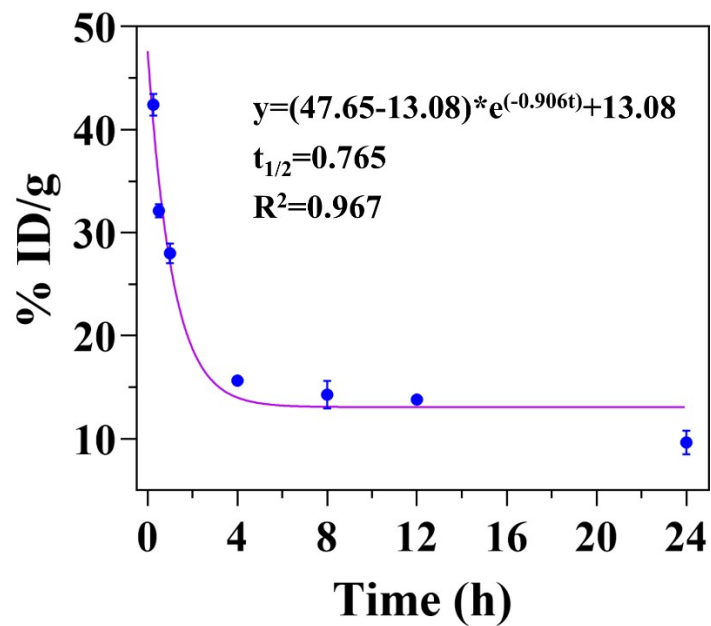


Figure S22. The concentration-time curve of Apt/siRNA@PT-ZIF-8 in mice after i.v. injection.

Blood biochemistry assays

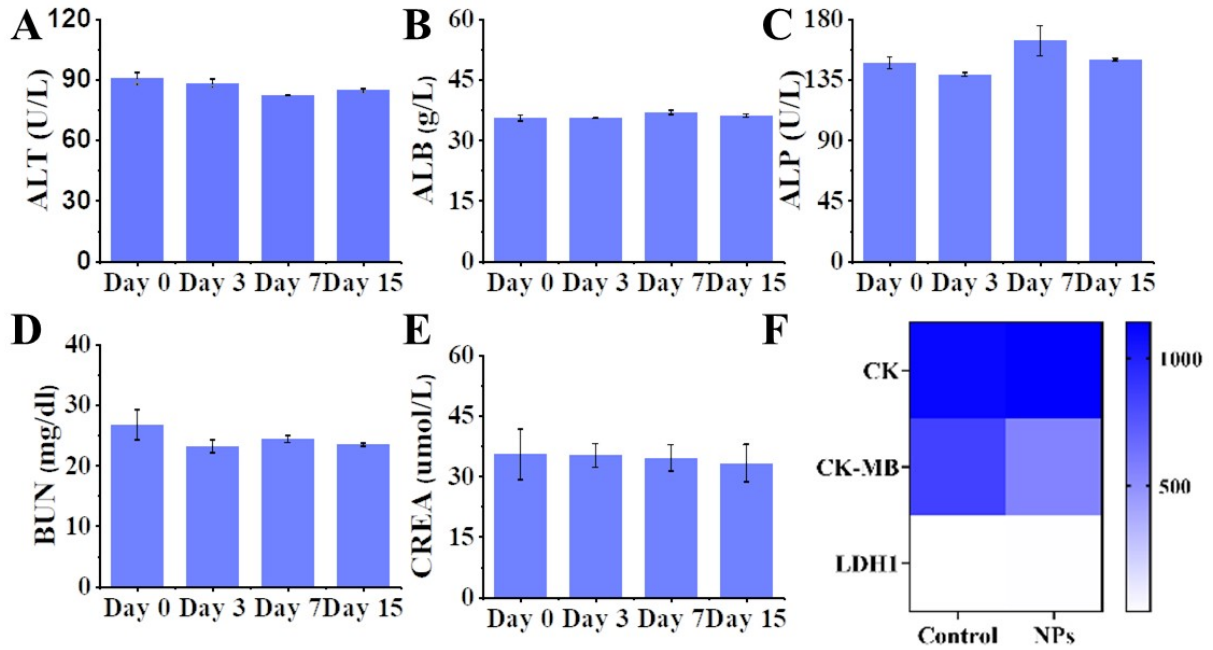


Figure S23. (A-C) Blood biochemistry assays of liver function markers: alanine aminotransferase (ALT), albumin (ALB), and alkaline phosphatase (ALP). (D, E) Blood biochemistry assays of kidney function markers: urea nitrogen (BUN) and creatinine (CREA). (F) Blood biochemistry assays of heart function markers: creatine kinase (CK), creatine kinase isoenzyme (CK-MB), and lactate dehydrogenase 1 (LDH1).

Histological analysis of major organs

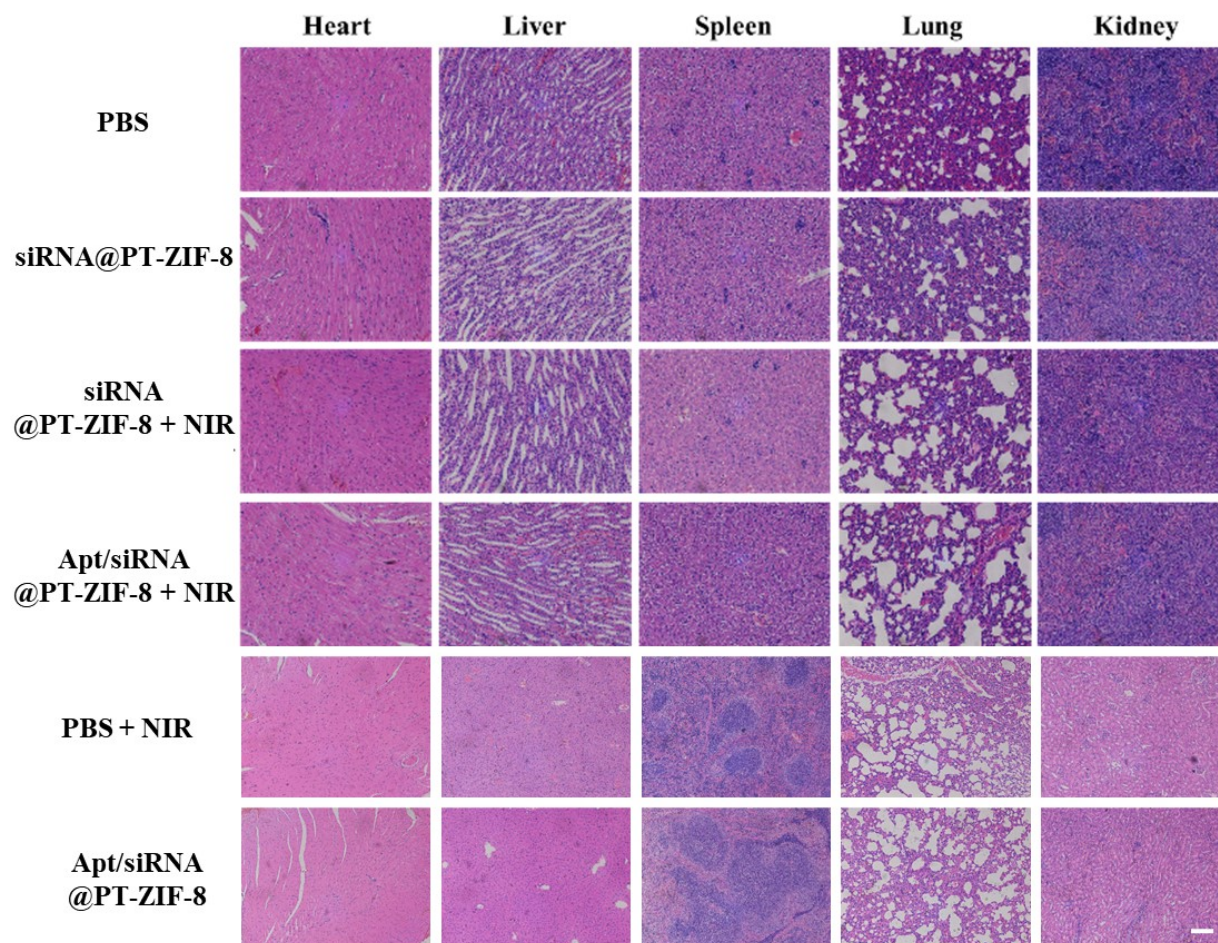


Figure S24. Histological analysis of major organs (hearts, livers, spleens, lungs, and kidneys) of tumor-bearing mice from different treated groups (PBS, siRNA@PT-ZIF-8, siRNA@PT-ZIF-8 + NIR, Apt/siRNA@PT-ZIF-8 + NIR, PBS + NIR, and Apt/siRNA@PT-ZIF-8). H&E staining images of major organs. Scale bar: 100 μ m.